Reinforcement of aligned cellulose fibres by lignin-polyester copolymers

Pei Lin Chee [1], Pek Yin Michelle Yew [1], Dan Kai [1]*, Xian Jun Loh [1]*

[1] Institute of Materials Research and Engineering (IMRE), A*STAR, 2 Fusionopolis Way, Innovis, no. 08-03, Singapore 138634 Singapore

* Corresponding Author

E-mail: kaid@imre.a-star.edu.sg, lohxj@imre.a-star.edu.sg

Abstract

With an ever-increasing attention on the climate change and the growing amount of plastic wastes generated, the search for an alternative to the petroleum-based plastics has never been as imperative. Inspired by the structure of natural wood, we aim to reproduce artificial equivalent using modified lignin and cellulose acetate. As natural wood are made up of an aggregation of fibres, electrospinning was used to produce the fibre component. Besides exploring the influence of various polymers on the properties of the eventual fibres, its properties were also examined in terms of its orientation – random and aligned. The addition of lignin copolymers was shown to remarkably improve the tensile strength and the Young's modulus of cellulose acetate fibres up to 500 % and 7000 % respectively. In contrast to the random fibres, the aligned fibres demonstrated better tensile strength and Young's modulus which could be attributed to the higher crystallinity. Among the fibres, the longitudinal aligned C.A. + Lig-PHB fibres exhibited the best tensile strength and Young's modulus which could be explored for load bearing applications.

Keywords: Lignocellulose, Ring-opening polymerization, poly(ε-caprolactone), poly(trimethylene carbonate), poly(3-hydroxybutyrate)

Introduction

Naturally occurring wood that are commonly obtained from trees are made up of an aggregation of fibres. Within each fibre strand, there exist smaller structures known as fibrils, which are crucial in providing mechanical stability and functioning as transport channels for water and minerals. These fibrillar structures in wood primarily consist of cellulose (38-50%), hemicellulose (23-32%) and lignin (15-25%), aptly illustrated in Figure 1 below.

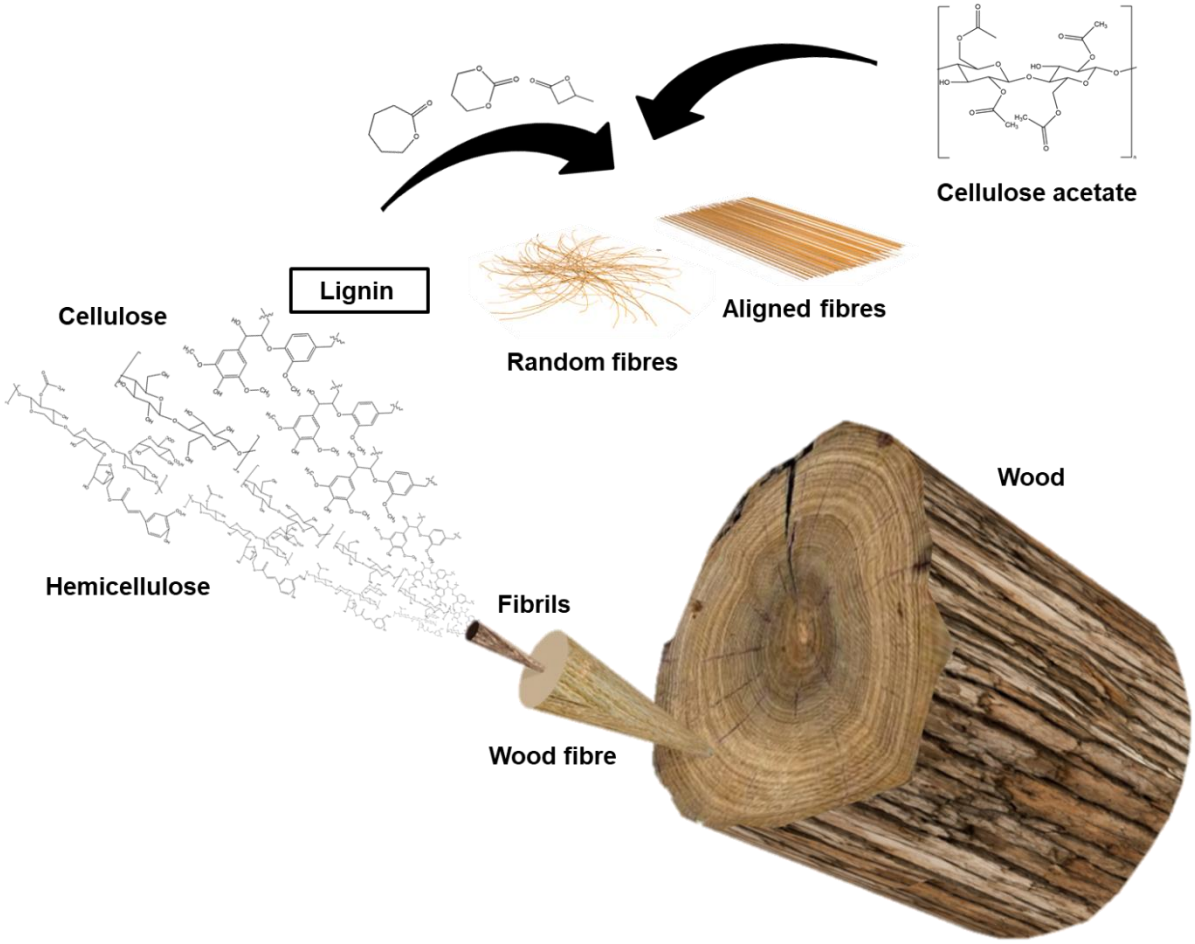

Figure 1 Schematic of modifying lignin extracted from wood with various monomers and subsequently blended with cellulose acetate to generate random and aligned fibres

With the fundamental structure of wood in mind, it is the aim of this study to reconstruct a similar structure using similar components (cellulose and lignin) via artificial means, to create a renewable alternative to the widely available petroleum-based plastics. Cellulose acetate is a modified natural polymer with tailorable properties depending on the degrees of substitution [1]. The most common type has good solubility in common solvents and melting properties [1]. Its applications are pretty widespread ranging from textiles, films to plastics and cigarette filters [1]. Lignin is currently being considered as industrial byproducts from paper and pulp industries but it exhibits various valuable traits such as high thermal stability, high carbon content, favorable stiffness and antioxidant activity [2-3]. Coupled the desirable properties with the high availability at low cost accentuates the alluring side of lignin, thereby highlighting it as a material worth exploring. The technique employed to construct the artificial wood fibres is electrospinning. In addition to being simple in process, it is also cost-effective in the generation of ultrafine polymeric micro/nanofibres [4]. Following the structure of the natural wood, cellulose acetate will thus be the main component of the fibre matrix, while lignin serves as structural reinforcement similar to its organic function.

However, lignin is widely reported to be incompatible with many polymer matrices [5-9] which limits its use. Chemical modification is a method that was found capable of overcoming this weakness. Specifically, grafting polymers onto lignin could improve its miscibility with other systems [5, 10]. Over the years, many techniques have been developed to graft polymers onto lignin which include atom transfer radical polymerization, polyurethane synthesis, ring-opening polymerization and reversible addition-fragmentation chain transfer [11-12]. For example, Qiu and team grafted functionalized polyethylene glycol onto alkali lignin via etherification to improve the reactivity of lignin [13]. Tang et al. performed atom radical polymerization to prepare rosin polymer-grafted lignin composites with excellent water resistance [14]. Si et al. demonstrated that the lignin-graft-polylactic

acid copolymers synthesized via ring-opening polymerization was capable of forming film with outstanding properties [15].

In this study, we synthesized a series of lignin copolymers via ring opening polymerization of ε-caprolactone or β-butyrolactone or trimethylene carbonate onto the lignin to improve its miscibility with cellulose acetate. For the examination of the polymer influence on the properties of the eventual fibres, the selected polymers differ in the stiffness with the toughest being poly(3-hydroxybutyrate) (PHB) follows by poly(ε-caprolactone) (PCL) and poly(trimethylene carbonate) (PTMC) [4, 16-18]. The Young's modulus and the tensile strength of bulk PHB was reported to be 3.0 GPa and 37.6 MPa respectively [19] (Supplementary Information). In comparison, PCL possesses a tensile modulus of 0.4 GPa and a tensile strength of 12.5 MPa [20] (Supplementary Information). PTMC has the weakest mechanical properties with the Young modulus and the ultimate tensile strength being 10.0 MPa and 0.8 MPa respectively [21] (Supplementary Information). In addition, the polymers have distinctive thermal, crystalline and mechanical properties. PHB has relatively high melting point in the range of 160 – 180 ˚C and it can crystalize rapidly [16]. On the contrary, PCL melts near 60 ˚C [22] while PTMC has a melting temperature at about 38 ˚C [23]. In order to reconstruct the structure of natural wood, the lignin copolymers were blended with cellulose acetate and electrospun into random and aligned fibres. Various characterizations were performed to examine the thermal stability and the mechanical properties of the fibres, thereby assessing its suitability as a replacement for petroleum based materials.

Materials and Characterizations

Materials

All chemicals were purchased from Sigma-Aldrich Chemicals except 1,3-dioxan-2-one which was obtained from TCI Chemicals. The chemicals were used as received unless noted otherwise. Kraft lignin (Mn = 1975 g mol^{-1}, Mw= 9599 g mol^{-1}) was dried at 110˚C overnight before use.

Grafting of polymers onto lignin

The lignin copolymers were synthesized using solvent free ring-opening polymerization. Each monomer (β-butyrolactone or ε-caprolactone or 1,3-dioxan-2-one) and the lignin in the mass ratio of 8 : 2 were weighed in a round bottom flask and purged with nitrogen at 105 ˚C. After purging for 30 minutes, 1,5,7-Triazabicyclo[4.4.0]dec-5-ene (TBD) catalyst (1 % molar ratio of monomer) was added. The mixture was stirred at 300 – 350 rpm overnight at 130 ˚C under an atmosphere of nitrogen gas. The reaction was allowed to cool down before it was quenched with dichloromethane and acetic acid. The unreacted monomers were segregated using precipitation with diethyl ether-methanol at the volume ratio of 2 to 1. The purified lignin copolymers were collected after drying.

Characterization of lignin copolymers

The successful chemical modification of lignin was verified with the use of fourier-transform infrared spectroscopy (FTIR) and proton nuclear magnetic resonance (^{1}H NMR) spectrometer. The FTIR spectra of the lignin copolymers were recorded for 128 scans from 4000 to 400 cm^{-1} with 1.0 cm^{-1} resolution whereas the ^{1}H NMR spectra of the copolymers dissolved in deuterated chloroform ($CDCl_3$) was obtained using JEOL 500MHz NMR spectrometer. The molecular weight and the polydispersity index (PDI) of polymer samples were acquired using the gel permeation

chromatography (GPC, Waters GPC system equipped with a 515 HPLC pump, Waters Styragel columns and a Waters 2414 refractive index detector). The eluent used for the test was tetrahydrofuran which was set at a flow rate of 1 ml/min at 40˚C. Monodispersed polystyrene standards were used to obtain the calibration curve. The thermal properties of the lignin copolymers were also investigated. The thermal stability of lignin copolymers was examined using the thermogravimetric analyser TGA Q500 by TA Instruments. The copolymers were heated up to 700 ˚C at a rate of 20 ˚C min^{-1} under dynamic nitrogen atmosphere (flow rate = 60 ml min^{-1}). Differential scanning calorimeter (DSC) thermal analysis was performed on a DSC (Q100, TA Instruments, USA) equipped with an autocool accessory and calibrated using indium. The following protocol was used for each sample: heating from room temperature to + 180 ˚C at 20 ˚C min^{-1}, holding at +180 ˚C for 5 min, cooling from +180 ˚C to -20 ˚C at 20 ˚C min^{-1}, and finally reheating from -20 to +180 ˚C at 20 ˚C min^{-1}. Melting temperature and enthalpy change were determined from the peak maxima and the endothermic melting peak respectively.

Electrospinning of fibres

A mixture of cellulose acetate and lignin copolymers was dissolved in 4:1 (v/v) chloroform-methanol to achieve 10% (w/v) solution. The mass ratio of cellulose acetate and lignin copolymers used for the electrospinning was 95:5. The solution was loaded into a syringe and collected onto an aluminum foil covered platform (20 cm away from the needle tip). The collected fibres were dried overnight under vacuum for future use. The random fibres were obtained with a set voltage 12 kV and a solution ejection rate 1 ml/h whereas higher set voltage and solution ejection rate (15 kV, 1.5 ml/h) were necessary to achieve aligned fibres. In addition, the aligned fibers were collected on the rotating drum (2000 rpm/min).

Characterization of fibres

The electrospun fibres were prepared into dog-bone shape and subjected to tensile tests using Instron 5569 Table Universal testing machine. Measurements were carried out at ambient temperature, with 10 N load cell and loading rate of 10 mm/min. Triplicate was tested for each type of lignin copolymers. Tensile stress, elongation and Young's modulus of the fibres were calculated from the stress-strain curve of each sample. The thermal properties of the electrospun fibres were studied with DSC and TGA using the aforementioned protocols and parameters. The surface topographies of the fibres were shown with the aid of scanning electron microscopy (SEM, JSM6700F, JEOL, Japan). The fibre diameters were determined from 50 random measurements per SEM image using image analysis software (Image J).

Results and Discussion

Synthesis of lignin copolymers

With the well-known fact that lignin has poor compatibility with most polymeric systems, various biodegradable polymers PCL, PHB and PTMC were sought with the aim to improve the miscibility of lignin with cellulose acetate. In this study, lignin was grafted with the polymers via the ring opening polymerization (Figure 2). ^{1}H NMR and FTIR were used to verify if the grafting was successful. The presence of lignin was identified by the peaks at 3.85 – 3.86 ppm which was associated to the methoxyl protons (Figure 2) [4, 24]. Characterized peaks of the PCL were also detectable at 2.29 ppm, 1.64 ppm, 1.37 ppm and 4.05 ppm which were attributed to α-, β-, γ- and

ε- methylene protons respectively [17, 24]. The chemical shifts noted at 1.26 ppm, 2.47 ppm and 5.23 ppm were assigned to the protons of $–CH_3$, $–CH_2$ and –CH in PHB chains respectively [17]. The peaks observed at 4.21 – 4.23 ppm and 2.02 – 2.05 ppm were accountable to the lateral and middle CH_2 proton in PTMC whereas the peak at 3.71 ppm was associated with the terminal hydroxy group [25]. Hence, the NMR results was indicative that the grafting was successful for all three copolymers.

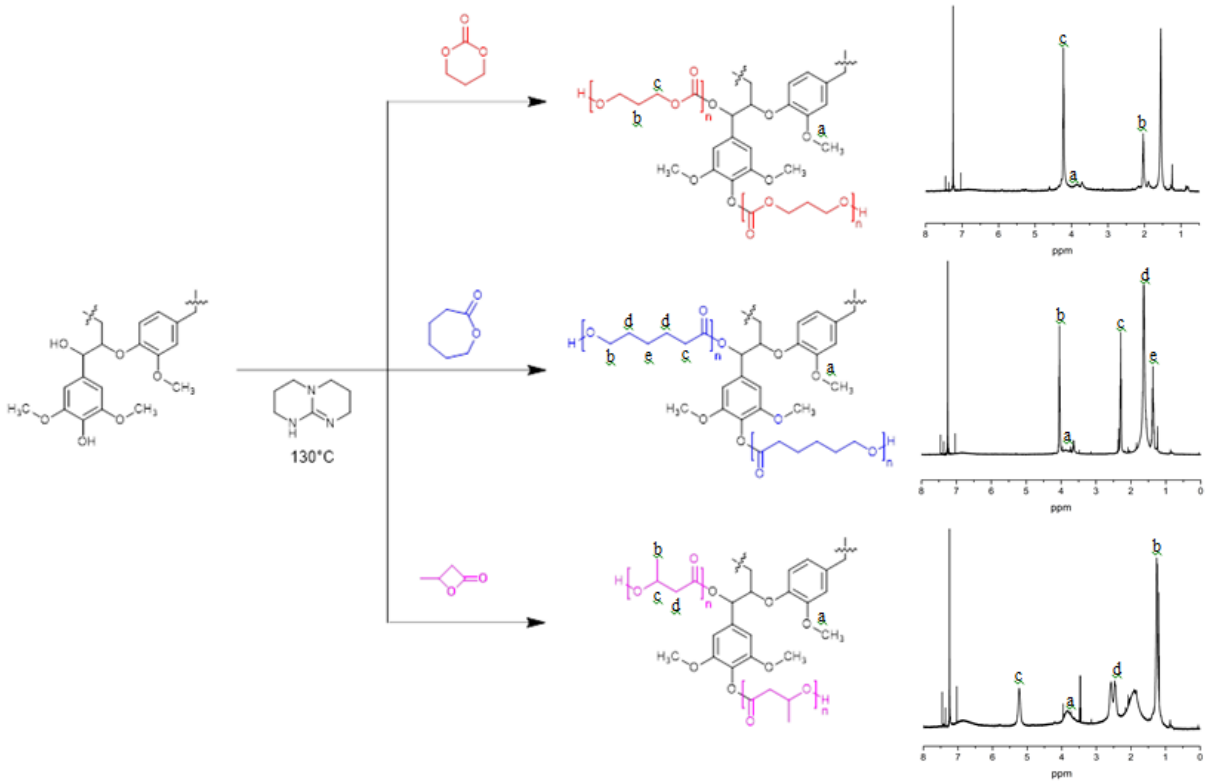

Figure 2 Ring opening polymerization of (top) trimethylene carbonate, (middle) ε-caprolactone and (bottom) β-butyrolactone on lignin using 1,5,7-Triazabicyclo[4.4.0]dec-5-ene as catalyst. The NMR spectra were displayed at the right.

With reference to FTIR spectrogram (Figure 3a) of Lig-PTMC, there were two distinct and intense peaks at 1747cm^{-1} and 1252 cm^{-1} that were not exhibited in the lignin spectrogram. Specifically, the 1747cm^{-1} peak was ascribed to the stretching frequency of carbonyl groups while the 1252 cm^{-1} peak proved the existence of a significant number of C-O bonds. These two intense peaks indicated that ester linkages were presented in the Lig-PTMC. Furthermore, the hydroxyl band at ~3400cm^{-1} was noted to be significantly reduced for Lig-PTMC as compared to lignin, with the C-H stretching peak at 2900 cm^{-1} being slightly more intense. Thus, the results signaled that the PTMC chains were successfully grafted onto lignin molecules. While there was no visible difference in the intensities of the hydroxyl bands between lignin and lignin copolymers (Lig-PHB and Lig-PCL), Lig-PHB had marginally more carbonyl stretching and Lig-PCL exhibited higher amount of C-H stretching at 2900 cm^{-1}. Therefore, Lig-PCL and Lig-PHB were also considered to have been synthesized successfully. However, the insignificant reduction in the intensities of the hydroxyl bands suggests that there were either fewer grafted sites or shorter chains in Lig-PCL and Lig-PHB as compared to Lig-PTMC. This hypothesis was validated by the molecular weight of the polymers as shown in Table 1. The molecular weight of Lig-PTMC was found to be 10,900 g mol^{-1}, which was much higher than Lig-PCL (2500 g mol^{-1}) and Lig- PHB (2600 g mol^{-1}). A possible explanation for the different grafting efficiency could be accounted to the catalyst used in the study. It is likely that TBD is more suitable for the ring opening polymerization of PTMC onto lignin. TBD is often used as a catalyst in the ring opening polymerization. Its efficiency as a catalyst was visible through the successful grafting of lactide onto lignin and the resultant lignin-g-poly(lactide acid) copolymer achieved a number-average molecular weight up to 11 kDa [26]. In another study, TBD catalyzed the ring opening reactions leading to a series of ethylene brassylate - ε-caprolactone copolymers with molecular weights ranging between 6.2 – 10.2 kDa [27]. However,

a better alternative to catalyze the grafting of PCL and PHB onto lignin might be Tin (II) 2-ethylhexanoate. Previously, our team demonstrated that it delivered high grafting of PCL and PHB onto lignin with molecular weights of the lignin copolymers found within 15.2 – 19.8 kDa [17].

The thermal properties of the lignin copolymers were characterized by TGA and DSC. Lig-PTMC demonstrated the best thermal stability as it experienced negligible weight loss up to around 220 ˚C (Figure 3b). While the other two lignin copolymers were less thermally stable as compared to lignin, it is noteworthy that all the lignin copolymers could withstand high temperature up to approximately 200 ˚C with minimal weight loss. This operating temperature range is sufficient for most applications. Hence, the larger decomposition at high temperature above 200 ˚C exhibited by the lignin copolymers should not undermine its uses. Different temperatures were required to cause the initial 5 wt% degradation for lignin copolymers as compared to lignin control (Table 1), which further indicated that the grafting of polymers onto the lignin was successful. It was noted that the temperature for Lig-PCL to experience 5 wt% degradation was pretty close to that of the lignin control. This observation could be explained by the possibility of fewer polymer chains were successfully grafted or the grafted polymer chains were short. If there were more occurrences of grafting or longer polymer chains, the temperatures recorded at 5 wt% decomposition of lignin copolymers should have been significantly higher than that of lignin [28]. The residue values obtained from the TGA test provide an indication of the degree of polymerization. From the results in Table 1, it could be interpreted that Lig-PCL had the lowest degree of polymerization given that its residue (52.6 wt%) measured at 600 ˚C was the closest to that of lignin control (54.3 wt%). In contrast, Lig-PTMC exhibited the greatest residue difference at 600 ˚C as compared to the lignin control suggesting that it had the highest degree of polymerization among the different lignin copolymers. The results was in good agreement with the FTIR results proposing that Lig-PTMC

had more grafted sites or longer polymer chains as compared to Lig-PCL and Lig-PHB. DSC results suggest that all copolymers are amorphous without any melting point (Figure 3c). This further proposes that the grafted polymer chains are not long enough to pack together in ordered regions to form the crystallites.

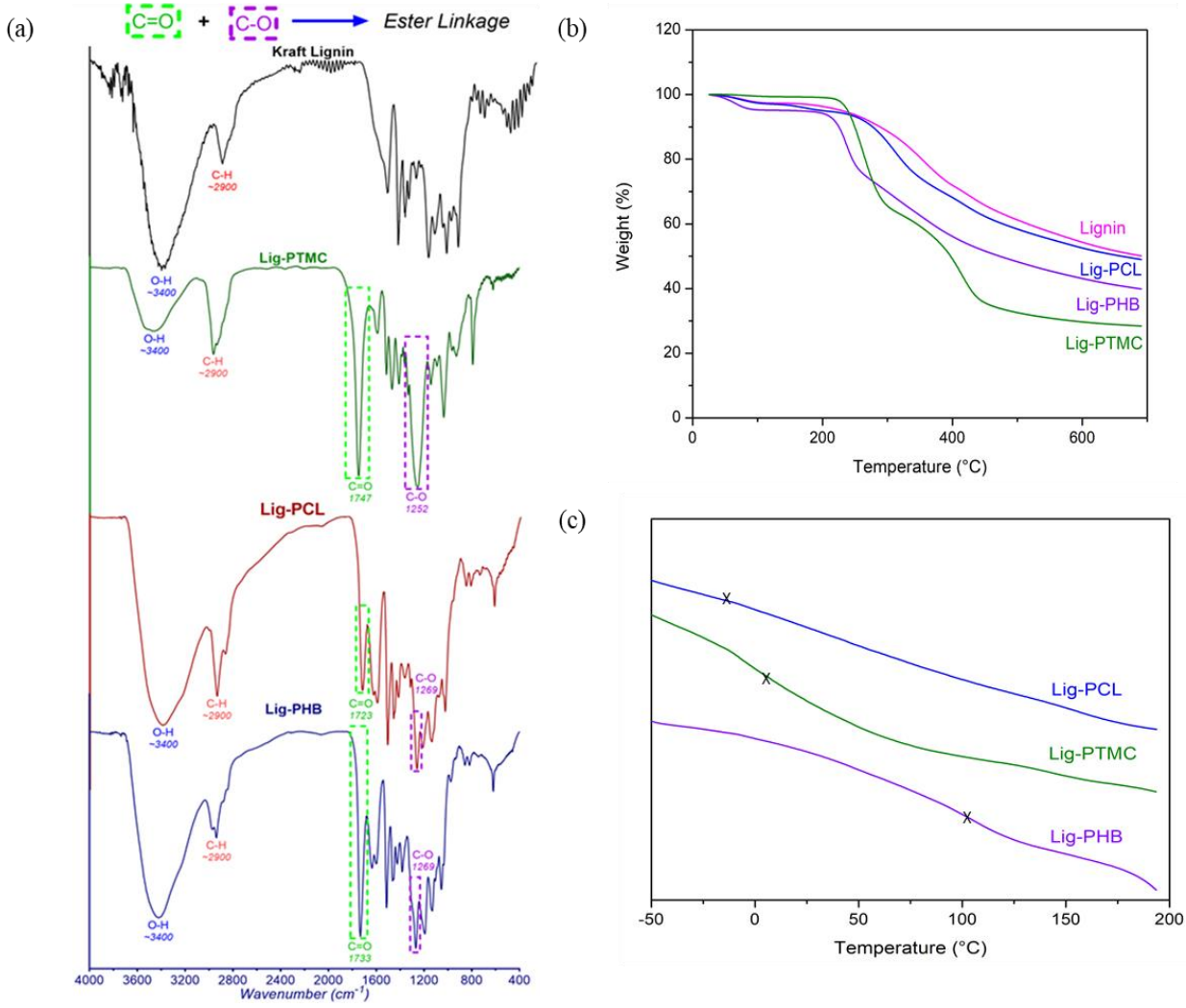

Figure 3 (a) FTIR spectra (b) TGA plots and (c) DSC thermograms of lignin and its copolymers

Table 1**:** Molecular characteristics and thermal properties of lignin and copolymers

Polymers	Lignin	Lig-PTMC	Lig-PCL	Lig-PHB
Feed ratio [Lig]:[Polymer]	100:0	95:5	95:5	95:5
Mn (g mol^{-1})	1975	10900	2500	2600
PDI	4.86	1.60	2.57	1.83
T_g (˚C)	164	8.17	- 6.60	106
$T_{95\%}$ (˚C)	230	239	261	224
Residue $_{600}$ (wt%)	54.3	29.7	52.6	43.1

Electrospinning of CA/lignin fibres

Lignin copolymers combined with cellulose acetate was engineered into composite fibres via electrospinning to recreate wood. In addition to the use of various polymers for the modification of lignin, the fibres were also electrospun into two orientations (random and aligned) to examine any possible difference in morphology and diameter of the collected fibres. The results were summarized in Figure 4. Uniform fibres were achieved without bead formation which indicated that the lignin had been successfully modified with the polymers and was miscible with cellulose acetate. With regards to the randomly oriented fibres, the incorporation of lignin copolymers into cellulose acetate fibres was found to have thinner diameter as compared to the cellulose acetate control (1.97 ± 0.68 μm). The difference in the diameter was noted to be as much as 60 % with the thinnest fibre being C.A. + Lig-PTMC which had a diameter of 0.76 ± 0.28 μm follows by C.A. + Lig-PHB (0.80 ± 0.12 μm) and C.A. + Lig-PCL (1.24 ± 0.62 μm). The trend observed could be explained by various factors such as the difference in the degree of polymerization, the viscosity and the conductivity of the solutions. The degree of grafting is closely related to the viscosity of the solution which was previously disclosed to exert an influence over the fibre diameter [29]. In fact, Frollini et al. demonstrated that the addition of lignin to recycled poly(ethylene terephthalate) (PET) increased the fibre diameter when the PET and lignin were left to stir in the trifluoroacetic acid for 72 hours [30]. When the preparation time was shortened to 48 hours, the electrospinning

solution was less viscous and insignificant difference in the fibre diameter was observed as compared to the PET control [30]. Another study revealed that the fibre diameter (m), h, could be estimated using the following equation:

$$\text{Eq.1} \quad \boldsymbol{h} = \left(\frac{\boldsymbol{\rho Q^3}}{\boldsymbol{2\pi^2 \frac{U^2}{RZ}}}\right)^{\frac{1}{4}} . \boldsymbol{Z^{-\frac{1}{4}}}$$

where Z, ρ, Q, U and R represent the distance from the nozzle to the collector (m), the density (kg/m^3), the flow rate (m^3/s), the applied voltage (V) and the electrical resistance of the jet (Ω) respectively [31]. According to the equation, a polymeric solution with higher conductivity, represented by 1/RZ, would generate thinner fibres. Hence, the fibre diameter is a function of many parameters and the resulting diameter would depend on the weightage of each variable.

Surprisingly, an opposite trend was observed when lignin copolymers and cellulose acetate were used together to produce aligned fibres. The blended aligned fibres were found with greater diameters than the cellulose acetate control with as much as 110 %, which was associated with C.A. + Lig-PTMC fibres (2.48 ± 0.75 μm). The diameters of aligned C.A. + Lig-PHB fibres and aligned C.A. + Lig-PCL fibres were measured to be 1.94 ± 0.88 μm and 1.86 ± 1.12 μm respectively. A possible explanation could be that the increment in the applied voltage used during the production of the aligned fibres amplified the effect caused by the conductivity. Considering the different conductivities of the solutions, the solution which had the greatest conductivity would therefore have the thinnest fibres. Hence, the thinnest fibres belonged to the cellulose acetate fibres. The least grafted C.A. + Lig-PCL based on the obtained results, that contained the highest

lignin content, exhibited the greatest conductivity among the different blended fibres. Hence, it had the thinnest fibres among the lignin copolymers fibres.

In order to achieve a certain degree of fibre alignment, the mandrel was optimized to rotate at a speed of at least 2000 rpm. A too high rotating speed was undesirable as it could lead to fibre breakage [32]. While it was noted that the rotating drums was far from ideal in collecting aligned fibres [33], the histograms in Figure 4 suggest that acceptably aligned cellulose acetate and C.A.+ Lig-PCL fibres were achieved in general direction of 0.51˚. In comparison, C.A. + Lig-PTMC and C.A.+ Lig-PHB fibres, collected in the general direction of -0.90˚ and 4.92˚ respectively, displayed less ideal fibre alignment. The phenomenon could be attributed to the disparity in the solution conductivities. Study revealed that a higher concentration of conducting polymer used in the electrospinning led to a better alignment of fibres observed [34]. Correspondingly, a solution that exhibits a higher conductivity would be expected to produce good fibre alignment as well. It was reported that introducing organic salt, such as benzyltriethylammonium chloride, improved the conductivity of the electrospinning solution and the fibre alignment [35]. This result could possibly be explained by the influence of solution conductivity on the shape of the electrostatic field, which eventually affects the alignment of the fibres [35]. Thus, this method could be explored to promote the alignment for C.A. + Lig-PTMC and C.A. + Lig-PHB fibres in the future.

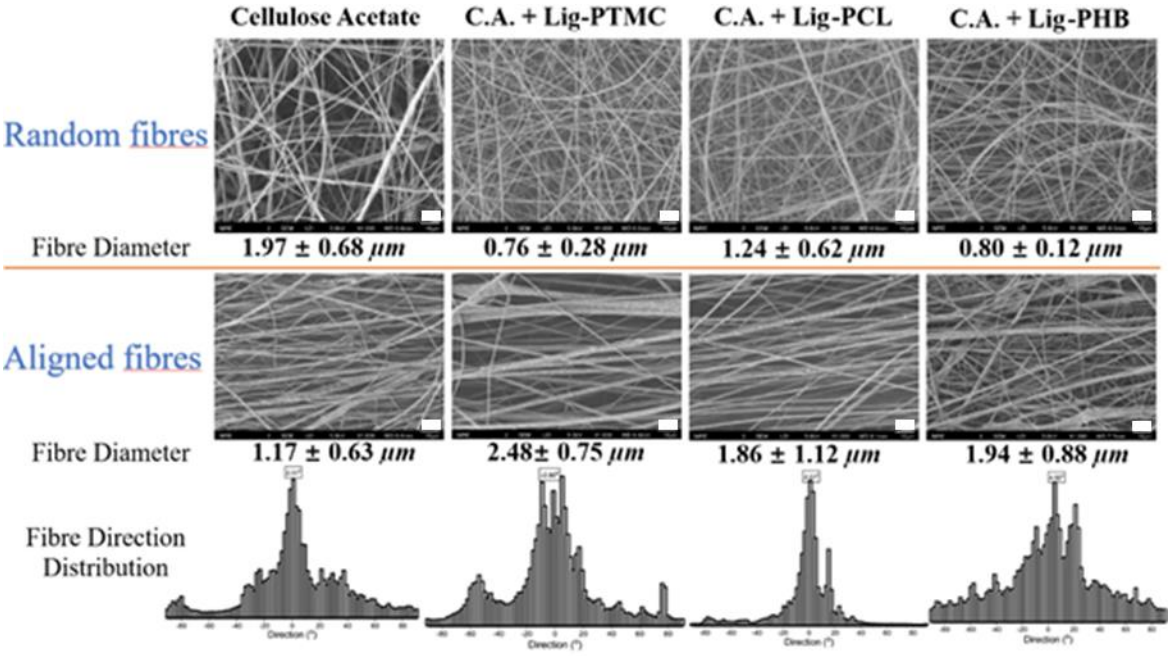

Figure 4 (top) SEM images of 10 % (w/v) electrospun fibres in 4:1(v/v) chloroform-methanol solvent. Scale bars = 10 µm. (bottom) Histograms which illustrate the distribution of fibres.

Mechanical properties of CA/lignin fibres

The tensile test results of the fibres were summarized in Table 2. The incorporation of lignin copolymers into the randomly aligned cellulose acetate fibres was generally found to enhance the Young's modulus and the tensile strength of the material but reduce its maximum strain. The results were not surprising as previous studies had shown that engineering lignin with cellulose generated material with better mechanical properties. For instance, Peng et al. discovered that the presence of lignin made a difference in the tensile strength and the toughness of cellulose nanopaper by 76 MPa and 6.9 MJ m^{-3} respectively [36]. Hu et al. successfully achieved lignin-cellulose composite with an exceptional isotropic tensile strength of 200 MPa using successive infiltration and mechanical hot-pressing treatments [37]. The latter study highlights that the

modification of lignin exposed more hydroxyl groups which promoted better interaction and compatibility [37] between the polymers and could be accounted for the higher tensile strength achieved. In another study, Kaewtatip et al. revealed that the esterification made lignin less densely interconnected and had a rougher surface, which together conferred it with better interaction with other polymers and improved mechanical properties [38]. The decline in the maximum strain of fibres due to the addition of the lignin copolymers was likely to be caused by stiffener function of the lignin [38]. It was also observed that the highest Young's modulus (11.9 ± 1.3 MPa) and tensile strength (1.1 ± 0.1 MPa) belong to C.A. + Lig-PTMC fibres follow by C.A. + Lig-PHB and C.A. + Lig-PCL fibres. The trend could be explained by the grafting degree. The grafting degree could be viewed as an indicator of the number of bonds present. Hence, the fibres with more grafting are expected to perform better mechanically. In addition, a higher degree of grafting suggests that there were more hydroxyl groups exposed for interaction which in turn, proposes enhanced compatibility and mechanical properties. Thus, C.A. + Lig-PTMC fibres, which were shown to have the most grafting, performed the best among the fibres. C.A. + Lig-PCL fibres exhibited the best strain follows by C.A. + Lig-PTMC fibres and C.A. + Lig-PHB fibres. The observed trend could be attributed to the combined effects of grafting degree and intrinsic property of the grafted polymer used. As aforementioned, a higher degree of grafting could be viewed as an indicator of the number of bonds present. The existence of more bonds implies that stronger force is needed to overcome the sum of bonds strength to stretch the fibres. Therefore, the fibres with more bonds are less stretchable given the same applied force. Another factor identified to have an influence over the maximum strain attainable by the fibres is the intrinsic property of the polymer. The selected polymers for the lignin modification differ in the stiffness with the toughest being PHB follows by PCL and PTMC. It is possible that this difference gets translated into the final fibres.

The illustrations in Figure 5 depict the orientation of fibres samples with reference to the vertical axis of the machine. When the tensile test was conducted in parallel with the fibres collection direction, on a rotating mandrel, the sample was described as aligned in the longitudinal direction (L). When the fibres was perpendicular to the collection direction, the collected fibres was known to be transversely aligned (T). Regardless of the alignment, the aligned fibres showed the same trends as the random fibres. All CA/lignin fibres achieved better tensile strength and Young's modulus but were weaker in the maximum strain attainable as compared to the CA fibres. In comparison, the aligned fibres performed differently to its random counterpart. The best fibres identified in terms of tensile strength and Young's modulus was C.A. + Lig-PHB fibres (A(L) 8.9 ± 2.4 MPa and 471.0 ± 56.4 MPa; A(T) 2.6 ± 0.4 MPa and 250.0 ± 18.8 MPa). The weakest fibres was C.A. + Lig-PTMC fibres (A(L) 5.9 ± 1.2 MPa and 238.0 ± 16.3 MPa; A(T) 0.5 ± 0.1 MPa and 14.5 ± 3.7 MPa). This could possibly be attributed to the intrinsic property being a more dominant factor for the aligned fibres. On the contrary, transversely aligned fibres displayed a different strain trend from the random fibres. The transversely aligned C.A. + Lig-PTMC fibres demonstrated the best elongation (12.2 %) whereas C.A. + Lig-PHB fibres performed the worst (1.51%). This is likely to be influenced heavily by the intrinsic property of the chosen polymers. It was noted that aligned fibres performed better quantitatively in tensile strength and Young's modulus as compared to the random fibres. A possible explanation could be the higher crystallinity of the aligned fibres as suggested by the data obtained from the thermal test. In contrast, the random fibres were noticed to be more flexible than the aligned counterpart.

Another finding was that the longitudinally aligned fibres achieved better tensile strength and Young's modulus as compared to transversely aligned fibres. The results were in good agreement with the work done by Staiger et al. [39]. They found that the tensile strength and the Young's

modulus of the cellulose composite were greater in the fibre direction by 87 MPa and 7.1 GPa respectively in relative to the fibre in the transverse direction [39]. The reason for the difference is probably due to the anisotropic characteristics [39] of the cellulose acetate fibres. There were different results for the strain to failure. The reason for the observed phenomenon is unclear. Among the fibres, longitudinally aligned C.A. + Lig-PHB fibres achieved the highest tensile strength (8.9 ± 2.4 MPa) and Young's modulus (471.0 ± 56.4 MPa) whereas random C.A. + Lig-PCL fibres attained the best strain (31.1 ± 6.9 %). It is worth noting that the increment of the tensile strength and the Young's modulus demonstrated by longitudinally aligned fibres exceeded 100% of that of the cellulose acetate fibres despite the inclusion of only 5 % of the lignin copolymers. In fact, some of the fibres even experienced an improvement of up to approximately 500 % and 7000 % for the tensile strength and the Young's modulus respectively. While the random C.A. + Lig-PCL fibres exhibited the best strain to failure among the fibres, it was still worse off than the cellulose acetate control but this decline was unavoidable due to the stiffener function of lignin.

It was reported that the strength and the modulus of radially cut nature wood were 4.46 MPa and 0.19 GPa respectively [40]. In contrast, nature wood cut in the longitudinal direction was found with strength of 42.72 MPa and a modulus of 5.78 GPa [40]. A comparison of the data indicates that the strength of several attained fibres was comparable to that of the radially cut nature wood but was lower than the longitudinally cut nature wood. The same observation was noted for the Young's modulus. This could be attributed to the current inability to reconstruct the exact chemical bonds that are present in nature wood.

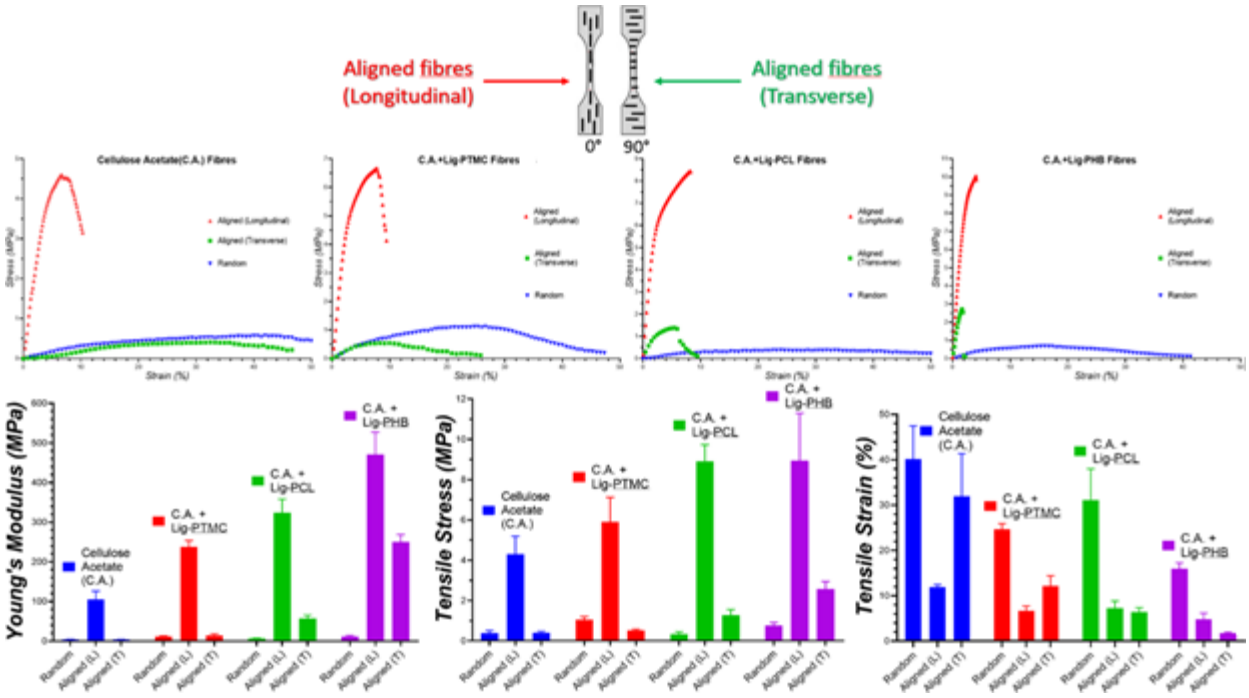

Figure 5 (top) Stress-strain curves of cellulose acetate fibres and its blended counterparts (bottom) Graphical comparison of the various mechanical properties of the fibres

Table 2: Mechanical properties of electrospun fibres (R, A(L) and A(T) represent random, longitudinally aligned and transversely aligned respectively)

Fibres Samples	Cellulose Acetate (C.A.)	C.A.+ Lig-PTMC	C.A.+Lig-PCL	C.A.+Lig-PHB
***E* (MPa)**				
R	3.7 ± 0.3	11.9 ± 1.3	6.3 ± 1.3	11.3 ± 2.9
A(L)	105.0 ± 20.7	238.0 ± 16.3	323.0 ± 34.6	471.0 ± 56.4
A(T)	3.4 ± 0.3	14.5 ± 3.7	56.5 ± 9.0	250.0 ± 18.8
***σ* (MPa)**				
R	0.4 ± 0.1	1.1 ± 0.1	0.3 ± 0.1	0.8 ± 0.2
A(L)	4.3 ± 0.9	5.9 ± 1.2	8.9 ± 0.8	8.9 ± 2.4
A(T)	0.4 ± 0.1	0.5 ± 0.1	1.3 ± 0.3	2.6 ± 0.4
***ε* (%)**				
R	40.1 ± 7.3	24.6 ± 1.3	31.1 ± 6.9	15.9 ± 1.3
A(L)	11.9 ± 0.6	6.7 ± 1.0	7.3 ± 1.6	4.8 ± 1.4
A(T)	32.0 ± 9.4	12.2 ± 2.3	6.4 ± 1.0	1.5 ± 0.2

Thermal properties of electrospun fibres

TGA result shows that the incorporation of lignin copolymers into cellulose acetate fibres did not significantly reduced the thermal stability of cellulose acetate. In fact, the fibres were applicable for usage up to around 300 ˚C (Supplementary Information, Figure S1). Among the three lignin copolymers used with cellulose acetate, C.A.+ Lig-PTMC fibres performed the best with slightly better thermal stability (Table 3).

The crystalline properties of the fibre were characterized by DSC. Melting temperatures of the electrospun fibres were obtained from the 1st heating cycle (Figure 6a and 6b). In general, the aligned fibres had lower melting points and higher enthalpy (ΔH) of fusion as compared to the random fibres of the same composition. The higher enthalpy of fusion exhibited by the aligned fibres suggests that it had a higher degree of crystallinity as more energy was required to melt it. Similar finding was acquired by Focarete et al.. They reported that the aligned poly(ethylene oxide) fibres had a greater degree of crystallinity than its random counterparts [41]. In their study, Li et al. revealed that the alignment process by means of rotating mandrel could boost the degree of crystallization for the aligned fibres [42]. These results corroborated well with the mechanical results obtained. The greater tensile strength and Young's modulus achieved for the aligned fibres could be explained by the higher crystallinity [43-44]. For the second heating cycle, the T_g of cellulose acetate fibres was identified to be 187 ˚C which coincided well with the range reported in the literature review (~185.85 - 246.85˚C) [45]. There was no significant difference noted between the T_g of the cellulose fibres and the cellulose acetate-lignin copolymer fibres except for C.A. + Lig-PTMC fibres. Its T_g was identified to be slightly lower and it could be attributed to the combination effect of intrinsic property of PTMC and its grafting degree. PTMC has a glass transition temperature that is lower than the room temperature at about -14 ˚C [46] while lignin has a higher

glass transition temperature between 130 ˚C and 150 ˚C depending on the source [47]. As aforementioned, Lig-PTMC had the greatest grafting degree among the polymers which in turn, means that more PTMC was presented in a given amount as compared to the PCL and PHB. Considering high PTMC and low lignin content in the C.A. + Lig-PTMC fibres, the observed difference in the T_g could be understood.

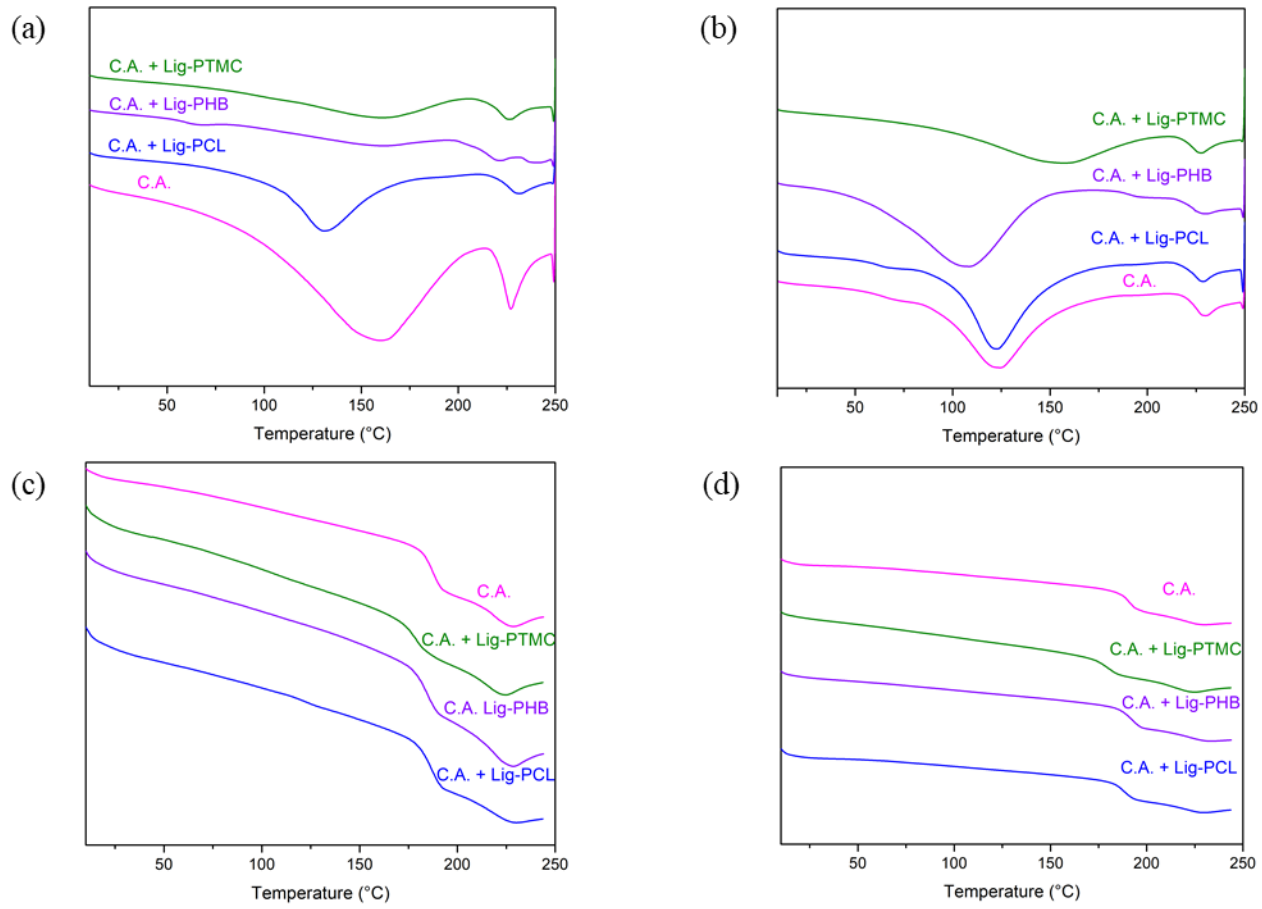

Figure 6 (a) and (b) illustrate the first heating cycle of random and aligned fibres respectively whereas (c) and (d) show the second heating cycle of random and aligned fibres respectively.

Table 3: Thermal properties of electrospun fibres (R and A represent random and aligned respectively)

Fibres	Cellulose Acetate (C.A.)		C.A.+ Lig-PTMC		C.A.+ Lig-PCL		C.A.+ Lig-PHB	
$T_{95\%}$ (˚C)	335		319		293		290	
Residue $_{600\ ^{\circ}C}$ (wt%)	13.9		11.3		5.0		13.5	
Orientation	R	A	R	A	R	A	R	A
Melting Points (˚C)	160	124	161	157	131	123	162	109
ΔH (J/g)	37.5	67.7	29.8	38.5	50.7	67.8	5.45	83.1
T_g (˚C) from 2nd heating run	187	190	179	179	186	188	185	193

Conclusion

In this work, we develop a facile method to use lignin, the industrial byproducts from paper and pulp industries, to add value to the cellulose acetate fibres. It was shown that the addition of a mere 5 % lignin copolymers led to the observation of up to 500 % fold increment in the tensile strength and up to 7000 % fold enhancement in the Young's modulus of the cellulose acetate fibres. Among the different fibres investigated, it was found that C.A. + Lig-PHB fibres generally achieved the best mechanical properties especially the longitudinal aligned ones. It attained 8.9 ± 2.4 MPa and 471.0 ± 56.4 MPa for tensile strength and Young's modulus respectively which highlights its potential to be further examined for load bearing applications. The remarkable improvement in the mechanical properties could be attributed to both the intrinsic property being a more dominant factor and the high crystallinity that was likely to be promoted during the alignment process.

Acknowledgement

This work was supported by Chia Sze Chen from Institute of Chemical and Engineering Sciences (ICES), A*STAR (Agency for Science, Technology and Research), Singapore. The authors also gratefully acknowledge the financial support from CDA (Project No. CDA 202D800033), Agency for Science, Technology and Research (A*STAR).

References

(1) Puls, J.; Wilson, S. A.; Hölter, D. Degradation of cellulose acetate-based materials: a review. *Journal of Polymers and the Environment* **2011,** *19* (1), 152-165.
(2) Wang, J.; Qian, Y.; Li, L.; Qiu, X. Atomic Force Microscopy and Molecular Dynamics Simulations for Study of Lignin Solution Self-Assembly Mechanisms in Organic–Aqueous Solvent Mixtures. *ChemSusChem n/a* (n/a),
(3) Zhou, Y.; Qian, Y.; Wang, J.; Qiu, X.; Zeng, H. Bioinspired Lignin-Polydopamine Nanocapsules with Strong Bioadhesion for Long-Acting and High-Performance Natural Sunscreens. *Biomacromolecules* **2020,** *21* (8), 3231-3241.
(4) Kai, D.; Jiang, S.; Low, Z. W.; Loh, X. J. Engineering highly stretchable lignin-based electrospun nanofibers for potential biomedical applications. *Journal of Materials Chemistry B* **2015,** *3* (30), 6194-6204.
(5) Hu, L.; Stevanovic, T.; Rodrigue, D. Unmodified and esterified K raft lignin-filled polyethylene composites: Compatibilization by free-radical grafting. *Journal of Applied Polymer Science* **2015,** *132* (7),
(6) Hilburg, S. L.; Elder, A. N.; Chung, H.; Ferebee, R. L.; Bockstaller, M. R.; Washburn, N. R. A universal route towards thermoplastic lignin composites with improved mechanical properties. *Polymer* **2014,** *55* (4), 995-1003.
(7) Kumar, A.; Tumu, V. R.; Chowdhury, S. R.; SVS, R. R. A green physical approach to compatibilize a bio-based poly (lactic acid)/lignin blend for better mechanical, thermal and degradation properties. *International journal of biological macromolecules* **2019,** *121*, 588-600.
(8) Wu, Y.; Qian, Y.; Lou, H.; Yang, D.; Qiu, X. Enhancing the Broad-Spectrum Adsorption of Lignin through Methoxyl Activation, Grafting Modification, and Reverse Self-Assembly. *ACS Sustainable Chemistry & Engineering* **2019,** *7* (19), 15966-15973.
(9) Yu, J.; Li, L.; Qian, Y.; Lou, H.; Yang, D.; Qiu, X. Facile and Green Preparation of High UV-Blocking Lignin/Titanium Dioxide Nanocomposites for Developing Natural Sunscreens. *Industrial & Engineering Chemistry Research* **2018,** *57* (46), 15740-15748.
(10) Fang, C.; Liu, W.; Qiu, X. Preparation of Polyetheramine-Grafted Lignin and Its Application in UV-Resistant Polyurea Coatings. *Macromolecular Materials and Engineering* **2019,** *304* (10), 1900257.

(11) Kai, D.; Zhang, K.; Jiang, L.; Wong, H. Z.; Li, Z.; Zhang, Z.; Loh, X. J. Sustainable and antioxidant lignin–polyester copolymers and nanofibers for potential healthcare applications. *ACS Sustainable Chemistry & Engineering* **2017,** *5* (7), 6016-6025.
(12) Wu, Y.; Qian, Y.; Zhang, A.; Lou, H.; Yang, D.; Qiu, X. Light Color Dihydroxybenzophenone Grafted Lignin with High UVA/UVB Absorbance Ratio for Efficient and Safe Natural Sunscreen. *Industrial & Engineering Chemistry Research* **2020**,
(13) Wang, S.; Liu, W.; Yang, D.; Qiu, X. Highly resilient lignin-containing polyurethane foam. *Industrial & Engineering Chemistry Research* **2018,** *58* (1), 496-504.
(14) Wang, J.; Yao, K.; Korich, A. L.; Li, S.; Ma, S.; Ploehn, H. J.; Iovine, P. M.; Wang, C.; Chu, F.; Tang, C. Combining renewable gum rosin and lignin: Towards hydrophobic polymer composites by controlled polymerization. *Journal of Polymer Science Part A: Polymer Chemistry* **2011,** *49* (17), 3728-3738.
(15) Liu, R.; Dai, L.; Hu, L.-Q.; Zhou, W.-Q.; Si, C.-L. Fabrication of high-performance poly (l-lactic acid)/lignin-graft-poly (d-lactic acid) stereocomplex films. *Materials Science and Engineering: C* **2017,** *80*, 397-403.
(16) Tang, X.; Thankappan, S. K.; Lee, P.; Fard, S. E.; Harmon, M. D.; Tran, K.; Yu, X., Polymeric biomaterials in tissue engineering and regenerative medicine. In *Natural and Synthetic Biomedical Polymers*, Elsevier: 2014; pp 351-371.
(17) Kai, D.; Chong, H. M.; Chow, L. P.; Jiang, L.; Lin, Q.; Zhang, K.; Zhang, H.; Zhang, Z.; Loh, X. J. Strong and biocompatible lignin/poly (3-hydroxybutyrate) composite nanofibers. *Composites Science and Technology* **2018,** *158*, 26-33.
(18) Jiang, T.; Zhang, G.; He, W.; Li, H.; Jin, X. The tissue response and degradation of electrospun poly (ε-caprolactone)/poly (trimethylene-carbonate) scaffold in subcutaneous space of mice. *Journal of Nanomaterials* **2014,** *2014*,
(19) Celarek, A.; Kraus, T.; Tschegg, E. K.; Fischerauer, S. F.; Stanzl-Tschegg, S.; Uggowitzer, P. J.; Weinberg, A. M. PHB, crystalline and amorphous magnesium alloys: Promising candidates for bioresorbable osteosynthesis implants? *Materials Science and Engineering: C* **2012,** *32* (6), 1503-1510.
(20) López-Rodríguez, N.; López-Arraiza, A.; Meaurio, E.; Sarasua, J. Crystallization, morphology, and mechanical behavior of polylactide/poly (ε-caprolactone) blends. *Polymer Engineering & Science* **2006,** *46* (9), 1299-1308.
(21) Guerin, W.; Helou, M.; Carpentier, J.-F.; Slawinski, M.; Brusson, J.-M.; Guillaume, S. M. Macromolecular engineering via ring-opening polymerization (1): L-lactide/trimethylene carbonate block copolymers as thermoplastic elastomers. *Polymer Chemistry* **2013,** *4* (4), 1095-1106.
(22) Schneiderman, D. K.; Hill, E. M.; Martello, M. T.; Hillmyer, M. A. Poly (lactide)-block-poly (ε-caprolactone-co-ε-decalactone)-block-poly (lactide) copolymer elastomers. *Polymer Chemistry* **2015,** *6* (19), 3641-3651.
(23) Sayyar, S.; Bjorninen, M.; Haimi, S.; Miettinen, S.; Gilmore, K.; Grijpma, D.; Wallace, G. UV cross-linkable graphene/poly (trimethylene carbonate) composites for 3D printing of electrically conductive scaffolds. *ACS applied materials & interfaces* **2016,** *8* (46), 31916-31925.
(24) Wang, J.; Tian, L.; Luo, B.; Ramakrishna, S.; Kai, D.; Loh, X. J.; Yang, I. H.; Deen, G. R.; Mo, X. Engineering PCL/lignin nanofibers as an antioxidant scaffold for the growth of neuron and Schwann cell. *Colloids and Surfaces B: Biointerfaces* **2018,** *169*, 356-365.

(25) Chen, X.; Wu, X.; Fan, Z.; Zhao, Q.; Liu, Q. Biodegradable poly (trimethylene carbonate-b-(L-lactide-ran-glycolide)) terpolymers with tailored molecular structure and advanced performance. *Polymers for Advanced Technologies* **2018,** *29* (6), 1684-1696.
(26) Chung, Y.-L.; Olsson, J. V.; Li, R. J.; Frank, C. W.; Waymouth, R. M.; Billington, S. L.; Sattely, E. S. A renewable lignin–lactide copolymer and application in biobased composites. *ACS Sustainable Chemistry & Engineering* **2013,** *1* (10), 1231-1238.
(27) Pascual, A.; Sardón, H.; Ruipérez, F.; Gracia, R.; Sudam, P.; Veloso, A.; Mecerreyes, D. Experimental and computational studies of ring-opening polymerization of ethylene brassylate macrolactone and copolymerization with ε-caprolactone and TBD-guanidine organic catalyst. *Journal of Polymer Science Part A: Polymer Chemistry* **2015,** *53* (4), 552-561.
(28) Liu, X.; Zong, E.; Jiang, J.; Fu, S.; Wang, J.; Xu, B.; Li, W.; Lin, X.; Xu, Y.; Wang, C. Preparation and characterization of Lignin-graft-poly (ε-caprolactone) copolymers based on lignocellulosic butanol residue. *International journal of biological macromolecules* **2015,** *81*, 521-529.
(29) Bazrafshan, Z.; Stylios, G. K. A novel approach to enhance the spinnability of collagen fibers by graft polymerization. *Materials Science and Engineering: C* **2019,** *94*, 108-116.
(30) de Oliveira Santos, R. P.; Rodrigues, B. V. M.; Santos, D. M. d.; Campana-Filho, S. P.; Ruvolo-Filho, A. C.; Frollini, E. Electrospun recycled PET-based mats: Tuning the properties by addition of cellulose and/or lignin. *Polymer Testing* **2017,** *60*, 422-431.
(31) Cramariuc, B.; Cramariuc, R.; Scarlet, R.; Manea, L. R.; Lupu, I. G.; Cramariuc, O. Fiber diameter in electrospinning process. *Journal of Electrostatics* **2013,** *71* (3), 189-198.
(32) Teo, W. E.; Ramakrishna, S. A review on electrospinning design and nanofibre assemblies. *Nanotechnology* **2006,** *17* (14), R89.
(33) Li, D.; Xia, Y. Electrospinning of nanofibers: reinventing the wheel? *Advanced materials* **2004,** *16* (14), 1151-1170.
(34) Zhang, J.; Qiu, K.; Sun, B.; Fang, J.; Zhang, K.; Hany, E.-H.; Al-Deyab, S. S.; Mo, X. The aligned core–sheath nanofibers with electrical conductivity for neural tissue engineering. *Journal of Materials Chemistry B* **2014,** *2* (45), 7945-7954.
(35) Wang, X.; Zhang, K.; Zhu, M.; Yu, H.; Zhou, Z.; Chen, Y.; Hsiao, B. S. Continuous polymer nanofiber yarns prepared by self-bundling electrospinning method. *Polymer* **2008,** *49* (11), 2755-2761.
(36) Wang, Q.; Du, H.; Zhang, F.; Zhang, Y.; Wu, M.; Yu, G.; Liu, C.; Li, B.; Peng, H. Flexible cellulose nanopaper with high wet tensile strength, high toughness and tunable ultraviolet blocking ability fabricated from tobacco stalk via a sustainable method. *Journal of Materials Chemistry A* **2018,** *6* (27), 13021-13030.
(37) Jiang, B.; Chen, C.; Liang, Z.; He, S.; Kuang, Y.; Song, J.; Mi, R.; Chen, G.; Jiao, M.; Hu, L. Lignin as a Wood-Inspired Binder Enabled Strong, Water Stable, and Biodegradable Paper for Plastic Replacement. *Advanced Functional Materials* **2020,** *30* (4), 1906307.
(38) Kaewtatip, K.; Thongmee, J. Effect of kraft lignin and esterified lignin on the properties of thermoplastic starch. *Materials & Design* **2013,** *49*, 701-704.
(39) Kröling, H.; Duchemin, B.; Dormanns, J.; Schabel, S.; Staiger, M. P. Mechanical anisotropy of paper-based all-cellulose composites. *Composites Part A: Applied Science and Manufacturing* **2018,** *113*, 150-157.
(40) Zhu, M.; Song, J.; Li, T.; Gong, A.; Wang, Y.; Dai, J.; Yao, Y.; Luo, W.; Henderson, D.; Hu, L. Highly anisotropic, highly transparent wood composites. *Advanced materials* **2016,** *28* (26), 5181-5187.

(41) Gazzano, M.; Gualandi, C.; Zucchelli, A.; Sui, T.; Korsunsky, A.; Reinhard, C.; Focarete, M. Structure-morphology correlation in electrospun fibers of semicrystalline polymers by simultaneous synchrotron SAXS-WAXD. *Polymer* **2015,** *63*, 154-163.
(42) Wang, X.; Zhao, H.; Turng, L.-S.; Li, Q. Crystalline morphology of electrospun poly (ε-caprolactone)(PCL) nanofibers. *Industrial & Engineering Chemistry Research* **2013,** *52* (13), 4939-4949.
(43) Pickering, K. L.; Sawpan, M. A.; Jayaraman, J.; Fernyhough, A. Influence of loading rate, alkali fibre treatment and crystallinity on fracture toughness of random short hemp fibre reinforced polylactide bio-composites. *Composites Part A: Applied Science and Manufacturing* **2011,** *42* (9), 1148-1156.
(44) Ero-Phillips, O.; Jenkins, M.; Stamboulis, A. Tailoring crystallinity of electrospun plla fibres by control of electrospinning parameters. *Polymers* **2012,** *4* (3), 1331-1348.
(45) Kamide, K.; Saito, M. Thermal analysis of cellulose acetate solids with total degrees of substitution of 0.49, 1.75, 2.46, and 2.92. *Polymer Journal* **1985,** *17* (8), 919.
(46) Zhao, L.; Tian, X.; Liu, X.; He, H.; Zhang, J.; Zhang, R. Miscibility and isothermal crystallization behavior of poly (butylene succinate-co-adipate)(PBSA)/poly (trimethylene carbonate)(PTMC) blends. *Journal of Macromolecular Science, Part B* **2016,** *55* (6), 591-604.
(47) Li, W.; Sun, N.; Stoner, B.; Jiang, X.; Lu, X.; Rogers, R. D. Rapid dissolution of lignocellulosic biomass in ionic liquids using temperatures above the glass transition of lignin. *Green Chemistry* **2011,** *13* (8), 2038-2047.